

Supplementary materials for the article

Determination of Mn Valence States in Mixed-Valent Manganates by XANES Spectroscopy

ALAIN MANCEAU,¹ MATTHEW A. MARCUS,² AND SYLVAIN GRANGEON¹

¹ISTerre, CNRS and Université de Grenoble 1, F-38041 Grenoble Cedex 9, France.

²Advanced Light Source, Lawrence Berkeley National Laboratory, One Cyclotron Road, Berkeley, CA 94720, USA

Pre-edge Background Subtraction and Post-edge Normalization

The usual procedure for subtracting a pre-edge linear background from XANES or EXAFS data involves choosing a line or polynomial which passes through the data at the lowest energies. However, the rise of the edge (or pre-edge) has a tail which extends far into the pre-edge region. What is often done, then, is to estimate "by eye" what that tail looks like and to subtract a pre-edge line which fits under it with the exclusion of the tail. Instead, both the tail and a linear pre-edge were fitted as:

$$y(E) = \frac{a}{E_0 - E} + b + c(E - E_0)$$

where E_0 , a , b , and c are parameters, and the fit is done over a user-selected range which generally comes up half or a third of the way up the first pre-edge rise (Fig. S1). The linear term was then subtracted as the pre-edge background. In fluorescence data for which the elastic contribution "leaks" into the fluorescence channel below the edge, another term was added:

$$y(E) = \frac{a}{E_0 - E} + b + c(E - E_0) + \frac{d}{(E - E_f)^4}$$

to approximate the upward curve generated by the elastic contribution being picked up by the tail of the detector response. In this case, E_f is the center of the detector passband. This extra term was not used for electron-yield data, which constitutes most of the database.

After pre-edge subtraction, a line was fitted through the data ranging from an energy of about 6600eV to the end of the data, chosen "by eye" so that the resulting normalized data (pre-edge subtracted divided by post-edge line) oscillates around one. The undoubted subjectivity of this procedure was mitigated in the Combo fits by allowing a slope as a free parameter. To do this, the weighted sum of chosen references was multiplied by a term $1 + \alpha(E - E_1)$ where α is a free parameter and E_1 is the energy for the start of data. This procedure largely compensates for the arbitrariness of the post-edge slope.

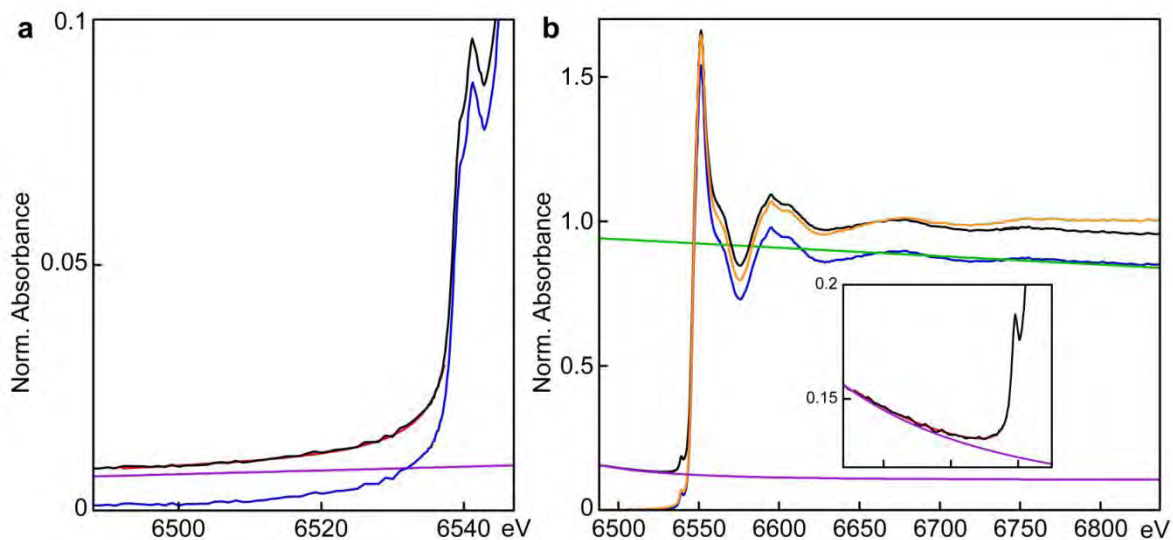


Figure S1. (a) Pre-edge normalization illustrated for a typical electron-yield data. (b) Pre- and post-edge normalization for a typical fluorescence data. Black: raw data, red: fit to pre-edge plus edge rise, purple: pre-edge line to be subtracted, blue: pre-edge normalized spectrum, green: post-edge line, orange: final pre- and post-edge normalized spectrum.

Principal Component Analysis

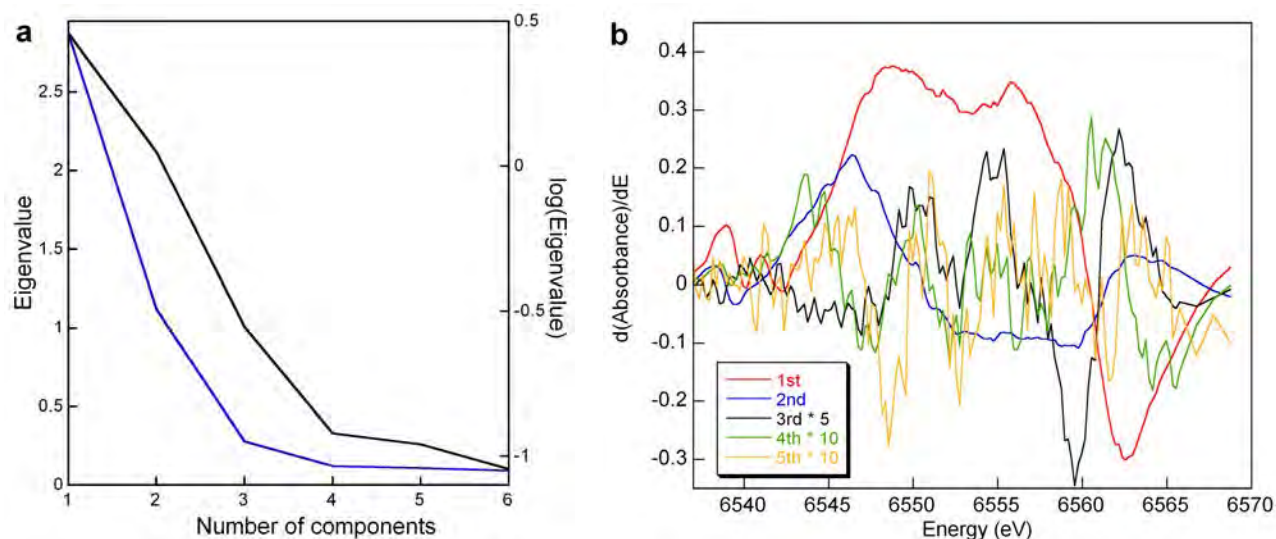


Figure S2. (a) Decline of the eigenvalues (λ) from the PCA in the 6535-6570 eV interval of the XANES derivatives for the twelve mixed-valent tectomanganates and phylломanganates with no or little layer Mn^{3+} . (b) First five principal components weighted by eigenvalues (λ). For clarity, the amplitudes of the 3rd, 4th, and 5th components have been multiplied by 5, 10, and 10, respectively. PCA identifies three orthogonal components.

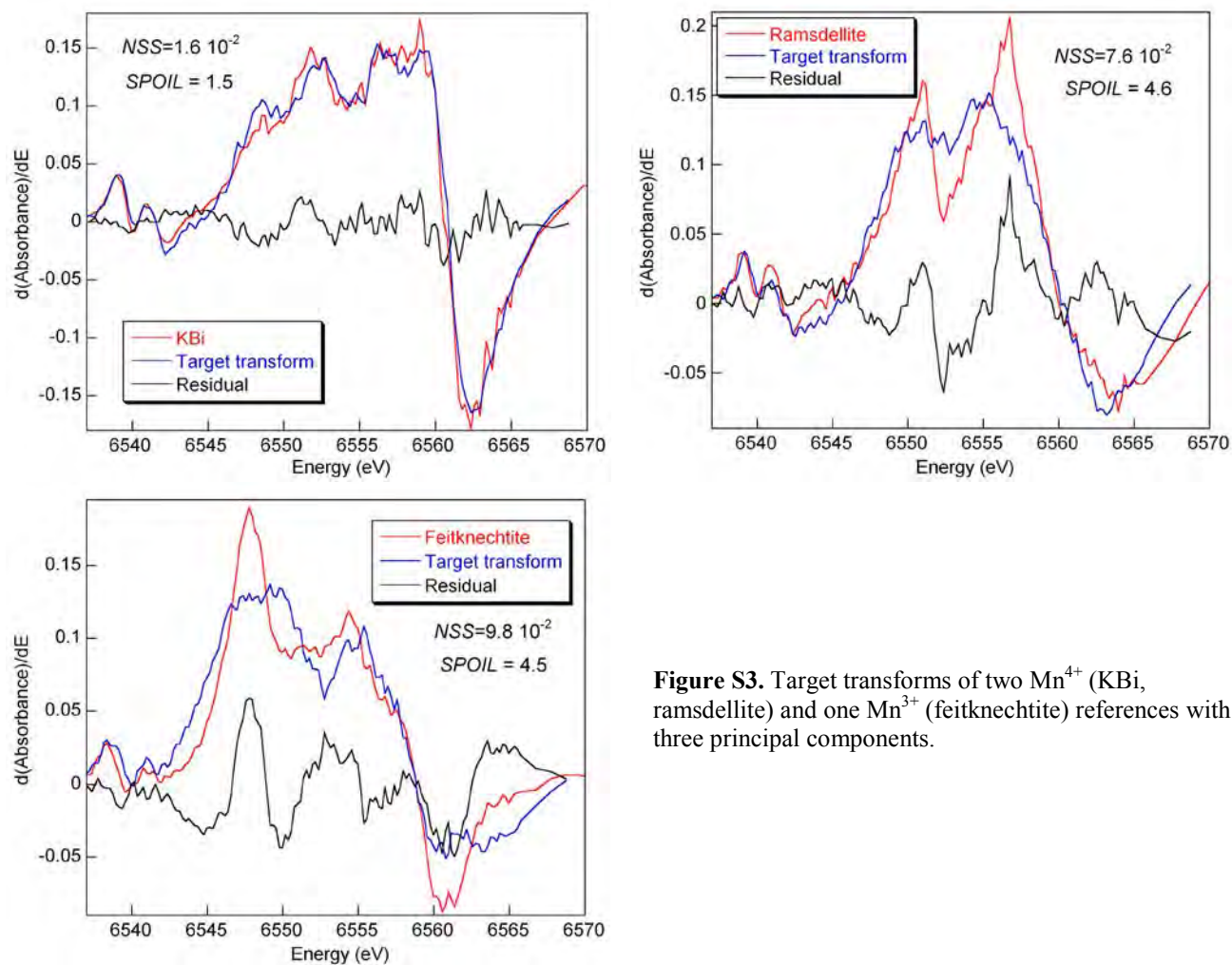


Figure S3. Target transforms of two Mn^{4+} (KBi , ramsdellite) and one Mn^{3+} (feitknechtite) references with three principal components.

The Combo Method

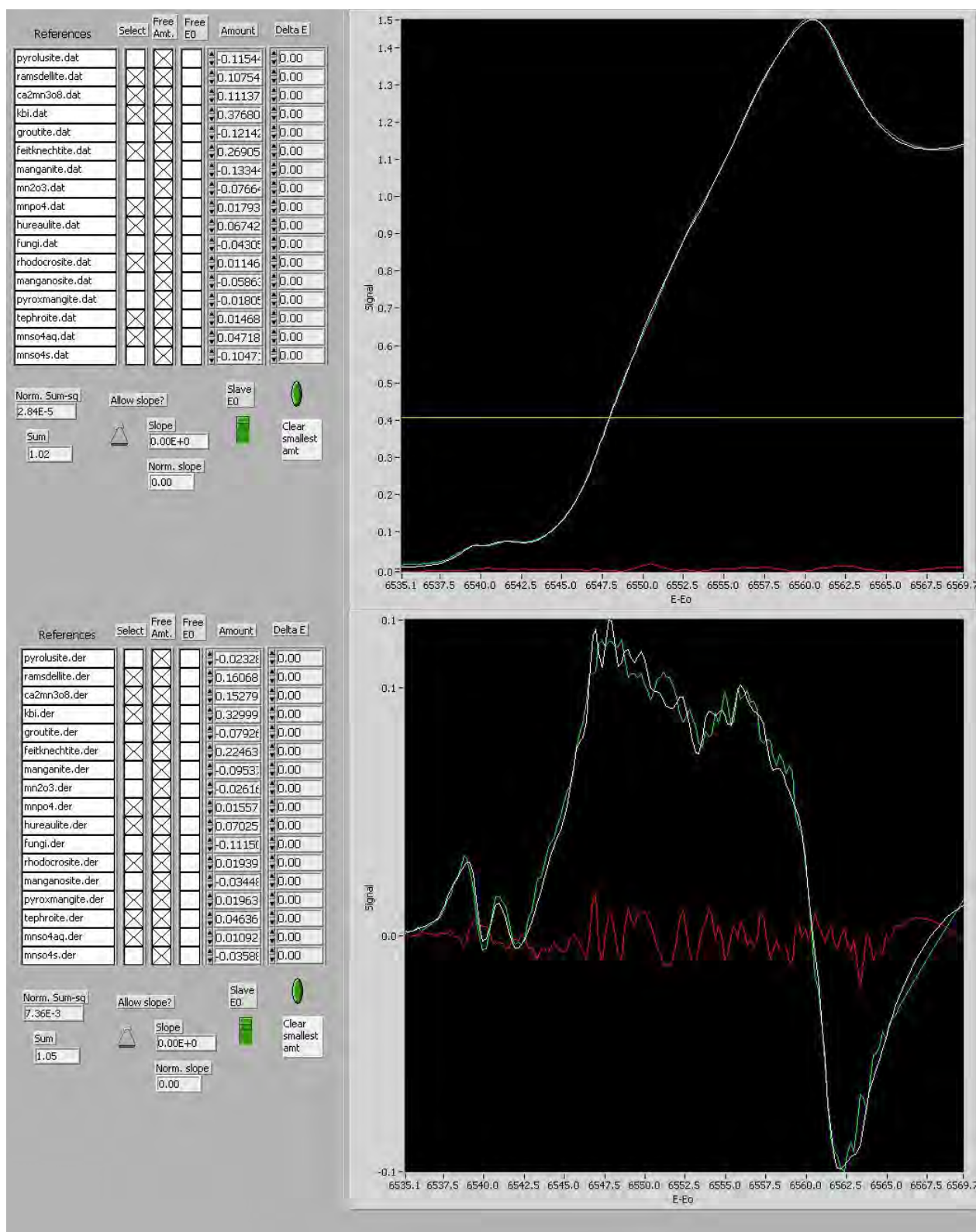


Figure S4. Linear combination fits of the XANES and derivative spectra for KR21-2 with the Combo method and the “Linear Fit w overabsorption” software from beamline 10.3.2 at the Advanced Light Source (<http://xraysweb.lbl.gov/uxas/index.htm>).

Error bars on individual components in a Combo fit are irrelevant, since that is not what we are after. Further, the error will be highly correlated in that one can push on one component and pull on a couple of others and come up with almost the same fit. Thus, the only obvious way to evaluate the error inherent in the method is to try it out on as many known mixed-valent compounds as possible and see how well it works. Normal statistical methods do not really apply because they assume that the error comes from noise in the unknown data, rather than from an incomplete model.

Table S1. Results from the PCA of the derivatives for the twelve mixed-valent tectomanganates and phyllomanganates with no or little layer Mn^{3+} in the 6535-6570 eV interval.

PC ^a	Eigenvalue ^b	% of variance ^c	IND x 10 ^{3d}	NSS-Tot	% of variation ^f
1	2.87	85.8	2.93	0.14	-
2	1.12	13.1	1.14	1.3 10 ⁻²	91
3	0.28	0.8	0.94	5.4 10 ⁻³	58
4	0.12	0.1	1.07	3.9 10 ⁻³	28
5	0.11	<0.1	1.23	2.6 10 ⁻³	33
6	0.09	<0.1	1.53	1.9 10 ⁻³	27

^a Principal component number (C). ^b Values of the diagonal matrix in the PCA after consecutive elimination of the components. Eigenvalues rank PCs according to their importance to reproduce data. ^c Fraction of the derivative signal accounted for by the first N components out of a maximum of six:

$$f_c \equiv \|\vec{Y}^C\| / \|\vec{Y}\| = \sum_{c=1}^6 \Lambda_c^2 / \sum_{c=1}^N \Lambda_c^2 . \quad ^d \text{Malinowski (1977) indicator value. } ^e \text{Normalized sum-squared total} =$$

$\sum_{\text{spectra}} \sum_n [\text{data} - \text{fit}]^2 / \sum_{\text{spectra}} \sum_n [\text{data}]^2$. This parameter is the normalized sum-squared (NSS) residual of the entire set of data, taken as one. ^f Marginal variation of $NNS\text{-}Tot = [(NSS\text{-}Tot)_{i+1} - (NSS\text{-}Tot)_i] / (NSS\text{-}Tot)_{i+1}$.

Table S2. Results from target transformation and weight fractions of the pure-valence references from the Combo fit of XANES spectra and derivatives in the 6535-6570 eV interval.

XANES	REF4-1	REF4-2	REF4-3	REF4-4	Sum	REF3-1	REF3-2	REF3-3	REF3-4	REF3-5	Sum	REF2-1	REF2-2	REF2-3	REF2-4	REF2-5	REF2-6	REF2-7	REF2-8	Sum	Sum	NSS x 10 ⁵
Hollandite		0.493	0.123	0.204	0.820	0.035	0.024		0.135		0.194									0.00	0.99	8.28
Psilomelane		0.222	0.143	0.382	0.747		0.149			0.089	0.238									0.00	0.99	10.20
Todorokite_Japan		0.443	0.143	0.193	0.779		0.081		0.151		0.232									0.00	1.01	15.00
Todorokite_SAF		0.191	0.090	0.416	0.697		0.169		0.053	0.074	0.296									0.00	0.99	15.50
KBi8		0.113	0.029	0.688	0.830		0.108			0.052	0.160									0.00	0.99	1.17
HBi5		0.230	0.092	0.346	0.668		0.280			0.011	0.291							0.049		0.049	1.01	4.35
KR21-2		0.107	0.111	0.377	0.595		0.269			0.018	0.287	0.067		0.011			0.015	0.047		0.140	1.02	2.84
KR21-Cu-A		0.189	0.169	0.392	0.750		0.114			0.045	0.159			0.010		0.005		0.069		0.084	0.99	3.50
KR21-Cu-B				0.058	0.058		0.509		0.102		0.611		0.084	0.052		0.192				0.328	1.00	19.80
SP6-Cu-A	0.020	0.054	0.173	0.464	0.711			0.091	0.036		0.127			0.030		0.088	0.006	0.034		0.158	1.00	5.99
SP6-Cu-B	0.046			0.063	0.109		0.355		0.162		0.517		0.049	0.050		0.248				0.347	0.97	15.20
SP6-Cu-C				0.026	0.026		0.116		0.269		0.385		0.035	0.131		0.415				0.581	0.99	29.9
1 st derivative	REF4-1	REF4-2	REF4-3	REF4-4	Sum	REF3-1	REF3-2	REF3-3	REF3-4	REF3-5	Sum	REF2-1	REF2-2	REF2-3	REF2-4	REF2-5	REF2-6	REF2-7	REF2-8	Sum	Sum	NSS x 10 ³
SPOIL	6.0	4.6	13.1	1.5		9.4	4.5	7.2	5.0	10.3		5.4	4.7	5.0	13.0	7.3	7.8	5.5	5.4			
NSS x 10	1.9	0.8	1.6	0.2		2.1	1.0	1.3	2.3	3.6		1.1	1.1	3.3	5.6	1.9	2.5	1.6	1.4			
Hollandite		0.561	0.194	0.106	0.861	0.092			0.076		0.168					0.017				0.017	1.05	14.90
Psilomelane		0.317	0.221	0.289	0.827		0.086			0.074	0.160				0.002	0.017	0.018			0.037	1.02	16.50
Todorokite_Japan		0.528	0.192	0.097	0.817	0.107		0.036	0.080		0.223					0.006				0.006	1.05	16.50
Todorokite_SAF		0.278	0.190	0.308	0.776		0.135			0.099	0.234					0.021	0.009			0.030	1.04	18.80
KBi8		0.120	0.076	0.652	0.848		0.102			0.042	0.144			0.005			0.007			0.012	1.00	4.04
HBi5		0.287	0.137	0.292	0.716		0.221			0.030	0.251	0.004		0.016		0.024	0.030			0.074	1.04	10.20
KR21-2		0.161	0.153	0.330	0.644		0.225			0.016	0.241	0.070		0.019		0.020	0.046	0.011		0.166	1.05	7.36
KR21-Cu-A		0.228	0.184	0.374	0.786		0.066			0.052	0.118	0.036		0.014		0.013	0.035	0.011		0.109	1.01	7.95
KR21-Cu-B	0.081		0.048	0.032	0.161		0.443		0.051		0.494	0.127	0.115	0.021	0.014	0.079				0.356	1.01	11.60
SP6-Cu-A	0.044	0.097	0.270	0.374	0.785		0.056				0.056	0.006		0.031		0.045	0.018	0.072		0.172	1.01	12.10
SP6-Cu-B	0.091		0.105		0.196		0.380	0.002	0.027		0.409	0.112	0.142	0.009	0.034	0.060	0.007			0.364	0.97	12.90
SP6-Cu-C	0.008		0.069		0.077		0.189		0.129		0.318	0.128	0.162	0.088	0.036	0.117	0.036			0.567	0.96	22.30

NSS is the normalized sum-squared residual = $\sum_n [\text{data} - \text{fit}]^2 / \sum_n [\text{data}]^2$.

Table S3. Results from target transformation and weight fractions of the pure-valence references from the Combo fit of XANES spectra and derivatives in the 6521-6653 eV interval

XANES	REF4-1	REF4-2	REF4-3	REF4-4	Sum	REF3-1	REF3-2	REF3-3	REF3-4	REF3-5	Sum	REF2-1	REF2-2	REF2-3	REF2-4	REF2-5	REF2-6	REF2-7	Sum	Sum	NSS x 10 ⁵	Slope x 10 ⁴
Hollandite		0.493	0.093	0.230	0.816	0.031	0.018		0.149		0.198								0.000	1.01	7.40	-1.23
Psilomelane		0.251	0.158	0.354	0.763	0.123	0.046			0.056	0.225						0.003		0.003	0.99	8.95	1.67
Todorokite_Japan		0.442	0.130	0.208	0.780	0.002	0.079		0.150		0.231								0.000	1.01	11.80	-0.74
Todorokite_SAF		0.183	0.133	0.388	0.704	0.027	0.183			0.079	0.289								0.000	0.99	11.90	1.29
KBi8		0.136	0.034	0.669	0.839	0.068	0.017	0.034		0.036	0.155			0.002					0.002	1.00	1.93	0.66
HBi5		0.217	0.064	0.366	0.647		0.281		0.010	0.024	0.315		0.010					0.034	0.044	1.01	3.98	-0.70
KR21-2		0.131	0.157	0.339	0.627		0.256			0.007	0.263	0.041		0.010				0.091	0.142	1.03	3.00	-2.73
KR21-Cu-A		0.208	0.190	0.366	0.764	0.052	0.069			0.023	0.144			0.008				0.079	0.087	1.00	3.63	1.34
KR21-Cu-B				0.068	0.068		0.500		0.098		0.598		0.094	0.048		0.190			0.332	1.00	13.80	0.34
SP6-Cu-A		0.088	0.167	0.481	0.736		0.084		0.007		0.091			0.015		0.106		0.048	0.169	1.00	5.29	0.74
SP6-Cu-B	0.069		0.064		0.133		0.247	0.130	0.100		0.477	0.033		0.052	0.019	0.240		0.022	0.366	0.98	19.90	2.70
SP6-Cu-C				0.064	0.064		0.132		0.191		0.323	0.039		0.099		0.467			0.605	0.99	23.60	0.83
1 st derivative	REF4-1	REF4-2	REF4-3	REF4-4	Sum	REF3-1	REF3-2	REF3-3	REF3-4	REF3-5	Sum	REF2-1	REF2-2	REF2-3	REF2-4	REF2-5	REF2-6	REF2-7	Sum	Sum	NSS x 10 ³	
Hollandite		0.559	0.193	0.108	0.860	0.092			0.076		0.168					0.017			0.017	1.05	15.20	
Psilomelane		0.309	0.220	0.293	0.822		0.091			0.075	0.166					0.017	0.019		0.036	1.02	17.20	
Todorokite_Japan		0.526	0.193	0.097	0.816	0.108		0.035	0.079		0.222					0.005			0.005	1.04	17.30	
Todorokite_SAF		0.274	0.192	0.309	0.775		0.139			0.096	0.235					0.020	0.009		0.029	1.04	19.20	
KBi8		0.124	0.079	0.649	0.852		0.101			0.038	0.139			0.006	0.004		0.004		0.014	1.01	4.25	
HBi5		0.282	0.135	0.295	0.712		0.222			0.032	0.254	0.005		0.016		0.025	0.028		0.074	1.04	10.50	
KR21-2		0.158	0.152	0.331	0.641		0.225			0.017	0.242	0.070		0.019		0.020	0.044	0.013	0.166	1.05	7.50	
KR21-Cu-A		0.224	0.183	0.376	0.783		0.068			0.053	0.121	0.035		0.014		0.014	0.033	0.013	0.109	1.01	8.30	
KR21-Cu-B	0.080		0.047	0.033	0.160		0.442		0.052		0.494	0.127	0.115	0.021	0.013	0.079			0.355	1.01	11.80	
SP6-Cu-A	0.042	0.097	0.266	0.377	0.782		0.057				0.057	0.007		0.030		0.046	0.016	0.072	0.171	1.01	13.10	
SP6-Cu-B	0.090		0.104		0.194		0.381		0.028		0.409	0.111	0.143	0.010	0.033	0.059	0.008		0.364	0.97	13.70	
SP6-Cu-C	0.010		0.070		0.080		0.189		0.125		0.314	0.131	0.160	0.088	0.036	0.118	0.036		0.569	0.96	23.00	

Table S4. Fractional and average valence states of Mn obtained from the Combo fit of XANES spectra and derivatives in the 6521-6653 eV interval.

	Fractional Mn ⁴⁺		Fractional Mn ³⁺		Fractional Mn ²⁺		Average Mn valence	
	XANES	Structure	XANES	Structure	XANES	Structure	XANES	Structure/Titration
XANES								
Hollandite	0.80	-	0.20	-	-	-	3.80	3.75-3.83
Psilomelane	0.77	-	0.23	-	-	-	3.77	3.75-3.75
Todorokite_Japan	0.77	-	0.23	-	-	-	3.77	3.72-3.73
Todorokite_SAF	0.71	0.73	0.29	0.27	-	-	3.71	3.73
KBi8	0.84	0.92	0.16	0.08	-	-	3.84	3.87-3.92
HBi5	0.64	0.72	0.31	0.22	0.04	0.05	3.60	3.66
KR21-2	0.61	-	0.25	-	0.14	-	3.47	-
KR21-Cu-A	0.77		0.14		0.09		3.68	
KR21-Cu-B	0.07		0.60		0.33		2.74	
SP6-Cu-A	0.74		0.09		0.17		3.57	
SP6-Cu-B	0.14		0.49		0.38		2.76	
SP6-Cu-C	0.06		0.33		0.61		2.45	
1st derivative								
Hollandite	0.82	-	0.16	-	0.02	-	3.81	3.75-3.83
Psilomelane	0.80	-	0.16	-	0.04	-	3.77	3.75-3.75
Todorokite_Japan	0.78	-	0.21	-	-	-	3.78	3.72-3.73
Todorokite_SAF	0.75	0.73	0.23	0.27	0.03	-	3.72	3.73
KBi8	0.85	0.92	0.14	0.08	0.01	-	3.83	3.87-3.92
HBi5	0.68	0.72	0.24	0.22	0.07	0.05	3.61	3.66
KR21-2	0.61	-	0.23	-	0.16	-	3.45	-
KR21-Cu-A	0.77		0.12		0.11		3.67	
KR21-Cu-B	0.16		0.49		0.35		2.81	
SP6-Cu-A	0.77		0.06		0.17		3.60	
SP6-Cu-B	0.20		0.42		0.38		2.82	
SP6-Cu-C	0.08		0.33		0.59		2.49	

Table S5. Average valence states of Mn derived from the Combo method and the integration method proposed by Capehart et al. (1995). Values in bold denote the best agreement with titration/structure among the three methods.

	Structure/Titration	Combo ^a	Capehart ^b	Capehart ^c
Hollandite	3.75-3.83	3.81	3.69	3.69
Psilomelane	3.75-3.75	3.76	3.68	3.68
Todorokite_Japan	3.72-3.73	3.77	3.66	3.66
Todorokite_SAF	3.73	3.70	3.66	3.66
KBi8	3.87-3.92	3.84	3.72	3.72
HBi5	3.66	3.61	3.53	3.53
KR21-2	-	3.45	3.34	3.32
KBi10	3.67-3.75	3.69	3.63	3.63
TcBi	3.69	3.81	3.66	3.66
Lithiophorite	3.67-3.68	3.55	3.55	3.55
Hausmannite	2.67	2.76	2.73	2.66

^a Least-squares fit of the main edge in the 6535-6570 eV interval; ^b Calibration curve obtained with all pure valence Mn species: $v = 1.816 + 0.275 \times \Delta E$; ^c Calibration curve obtained with MnO, Mn₂O₃ and MnO₂ (pyrolusite): $v = 1.687 + 0.295 \times \Delta E$.

References

- Capehart, T.W., Herbst, J.F., and Pinkerton, F.E. (1995) X-ray-absorption edge shifts in rare-earth-transition-metal compounds. *Physical Review*, B52, 7907-7914.
- Malinowski, E.R. (1977) Determination of the number of factors and the experimental error in a data matrix. *Analytical Chemistry*, 49, 612-617.